Supporting Information

Structure Design of $NiCo_2O_4$ Electrodes for High Performance Pseudocapacitors and Lithium-Ion Batteries

Jun Pu,† Ziqiang Liu,† Zihan Ma, Jian Wang, Lei Zhang, Shaozhong Chang, Wenlu Wu, Zihan Shen,

Huigang Zhang*

National Laboratory of Solid State Microstructures, College of Engineering and Applied Sciences, and Collaborative Innovation Center of Advanced Microstructures, Nanjing University, Nanjing 210093, China

† These authors contribute equally to this work.

* Corresponding author. E-mail: hgzhang@nju.edu.cn.

Comparison of three types of current collectors and their configuration in electrodes

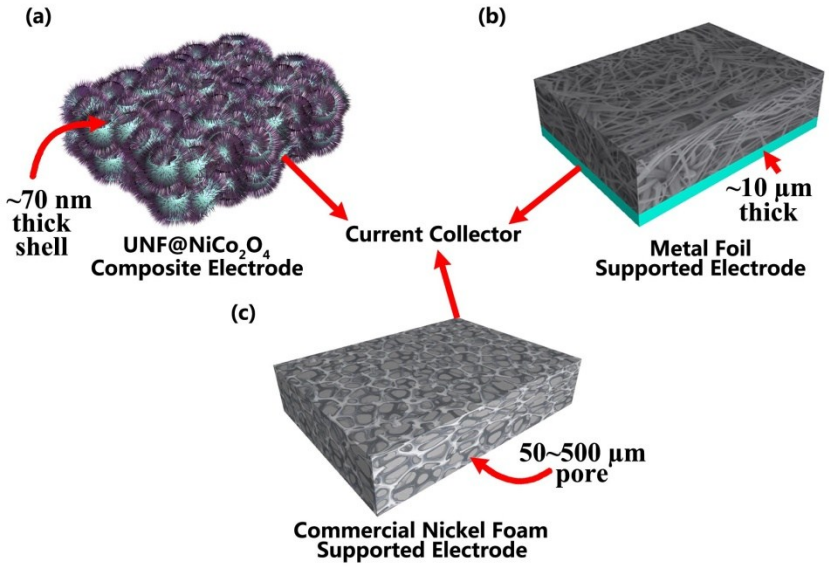

Fig. S1. Illustration of current collectors in (a) UNF@$NiCo_2O_4$ electrodes, (b) metal foil supported electrodes, and (c) commercial nickel foam supported electrodes. Note the characteristic sizes in the three current collectors.

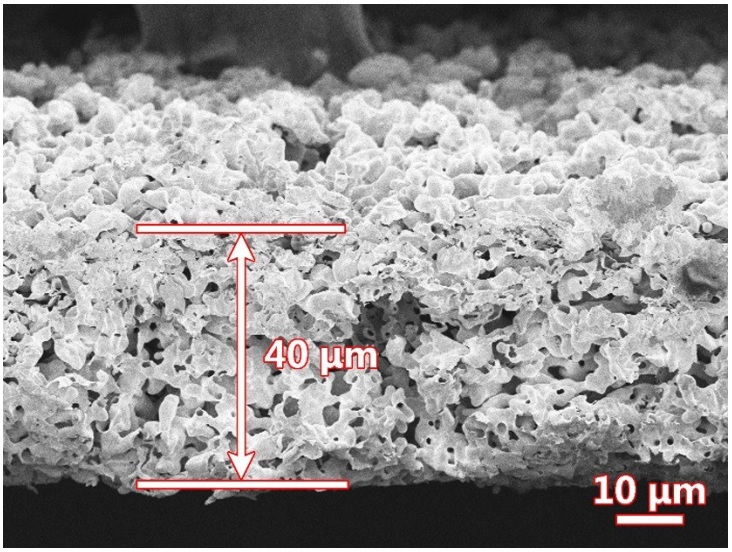

Fig. S2. SEM cross section image of UNF.

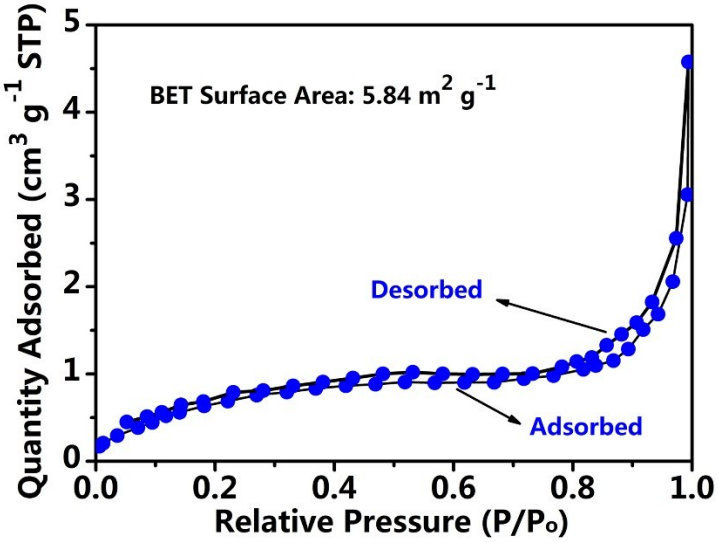

Fig. S3. N_2 adsorption-desorption isotherm of a UNF sample. The BET surface area of UNF is 5.84 m^2 g^{-1}

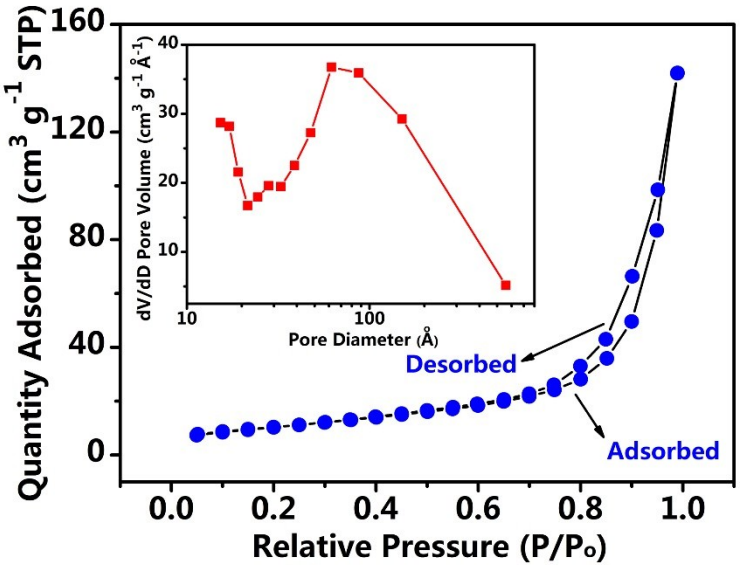

Fig. S4. N_2 adsorption-desorption isotherm of the as-prepared $NiCo_2O_4$ nanowires sample. The inset is the corresponding pore size distribution.

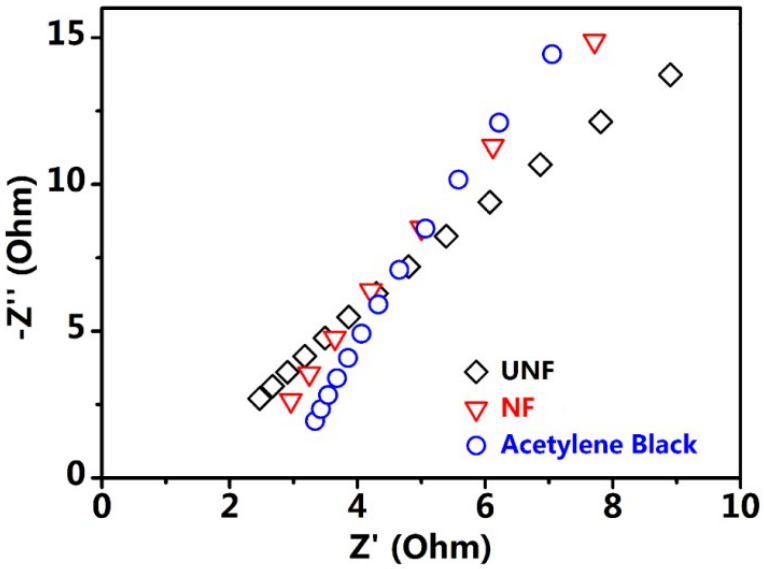

Fig. S5. High-frequency region of Nyquist plots.

Several typical commercial supercapacitors and Li-ion batteries and their components

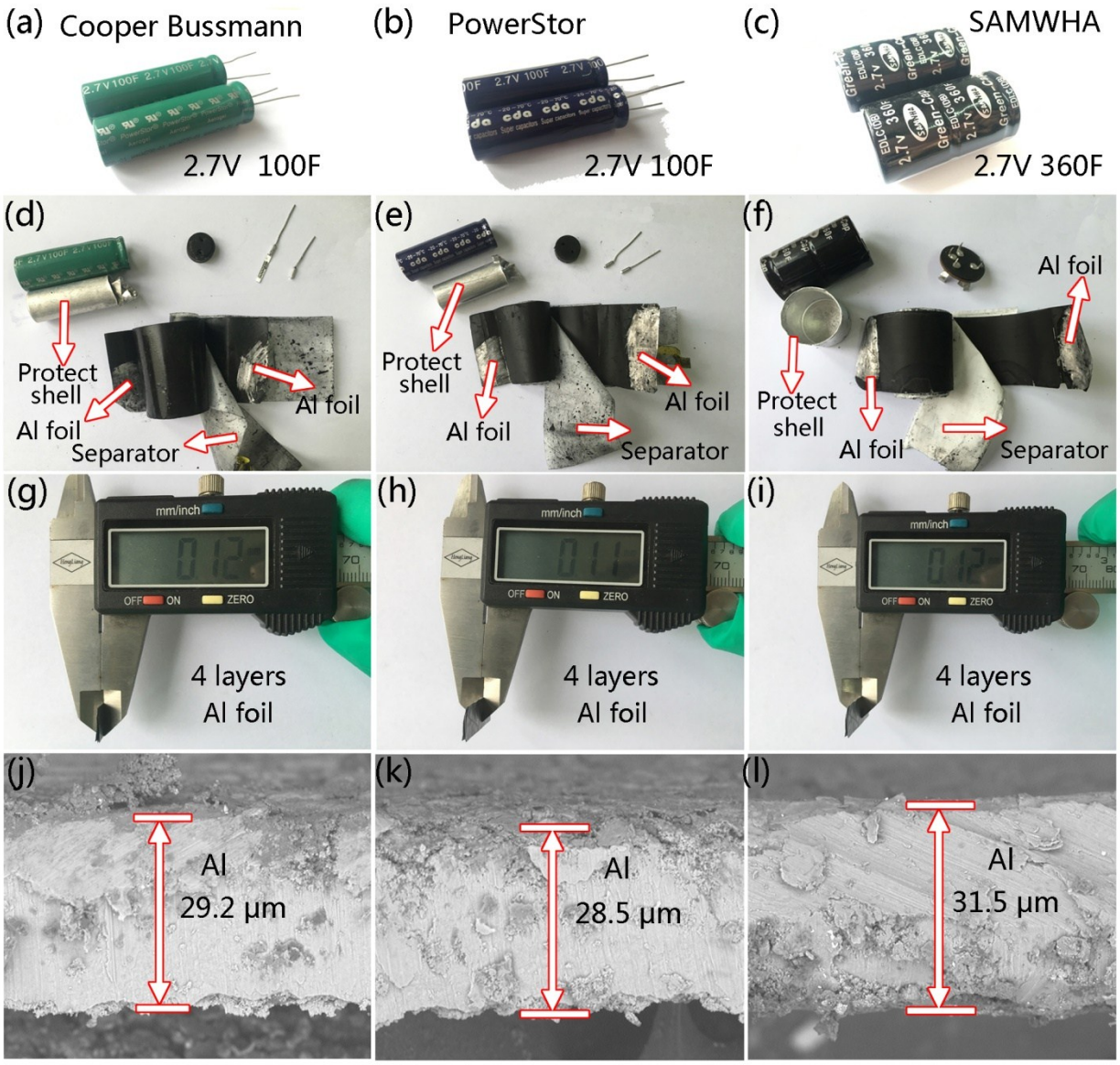

Fig. S6. Optical images of (a-c) three commercial supercapacitors and (d-e) their components after disassembly. (g-i) thickness measurements of four layer of their current collectors (Al foil). (j-l) SEM images of the three current collectors.

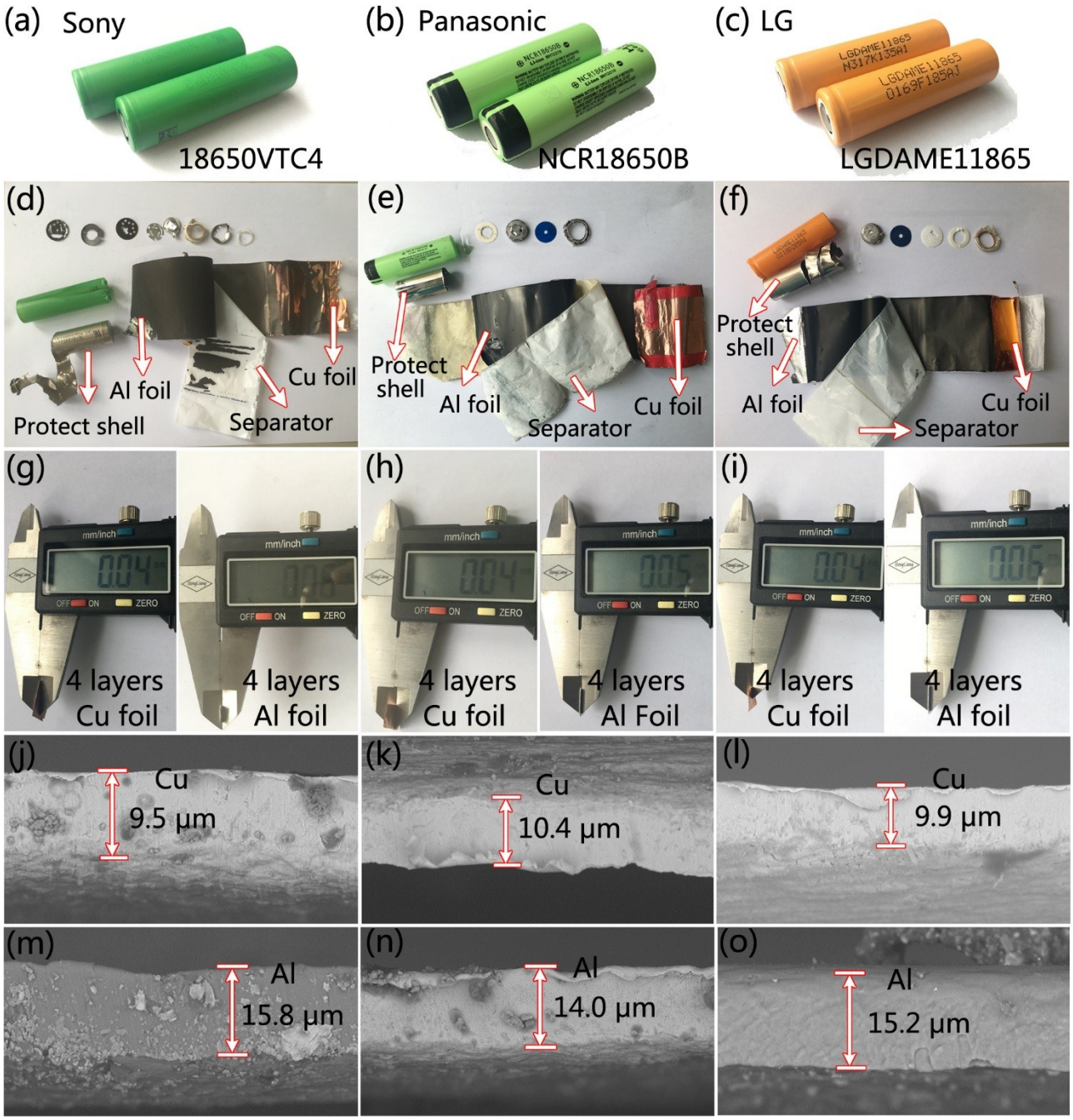

Fig. S7. Optical images of (a-c) three commercial Li-ion batteries and (d-e) their components after disassembly. (g-i) thickness measurements of their current collectors (Cu foil for anodes and Al foil for cathods). (j-l) SEM images of the anode current collectors. (m-o) SEM images of the cathode current collectors.

Summary of $NiCo_2O_4$ pseudocapacitors in literatures

Fig. S6 shows three commercial supercapacitors and their disassembled components. When supercapacitors are assembled, active materials slurries are usually coated on Al foil. Although the active material layer is conductive, a metal current collector is still required because the in-plane conductivity of active material layer is relatively too low to meet the requirements of high power applications. Another technical concern is that there are difficulties on welding carbonaceous materials and metallic tabs. Metal foil current collectors are easy to weld with metallic tabs. In Fig. S6j−l, the commercial supercapacitors use about 30 μm thick Al foils to conduct electrons in order to reduce internal resistance and enhance the power densities of supercapacitors. Because of the similar reasons, Li-ion batteries also require metal foils to collect electric currents. Fig. S7m−o show that about 15 μm thick Al foils are used in several typical commercial Li-ion battery anodes.

The electrode-based capacitance is lower than that of active materials basis. For practical applications, the total mass of electrodes including both active material layer and current collectors must be considered to fabricate high energy/power devices. Therefore, it is more reasonable to compare the specific capacitance of a real electrode on the basis of total mass. Table S1 summarizes the previous reports about supercapacitors using $NiCo_2O_4$ as the active materials. The current collectors used in the literatures are Al foil, Ni foam, carbon fiber network etc. Most of papers do not disclose the exact parameter of the current collectors. For the literatures using commercial nickel foam, we used the data (20 mg cm^{-2}) which are adopted from the widely-cited two papers about commercial nickel foam.[2,3] For carbon fiber network and other carbon based collectors, no information about the mass of current collectors is provided in the literatures. It is unable to estimate the electrode-based capacitance.

Table S1. Performance and parameters of previously reported $NiCo_2O_4$ pseudocapacitors.

$NiCo_2O_4$ Electrode Structure	Loading (mg cm^{-2})	Specific capacitance (active material basis) [a]	Specific capacitance (electrode basis) [b]	Cyclability	Ref.
Nanowires on UNF	6.0	1552 F g^{-1} at 1 A g^{-1}	1128 F g^{-1} at 0.8 A g^{-1}	83% after 5000 cycles	This work
Nanosheets on Ni foam	0.8	1450 F g^{-1} at 20 A g^{-1}	(56 F g^{-1} at 0.7 A g^{-1})	94% after 2400 cycles	4
Nanosheets on Ni foam	1.2	1743 F g^{-1} at 7 A g^{-1}	(99 F g^{-1} at 0.4 A g^{-1})	93% after 3000 cycles	5
Nanocyclobenzene on Ni foam	2.5	1545 F g^{-1} at 5 A g^{-1}	(172 F g^{-1} at 0.6 A g^{-1})	93% after 5000 cycles	6
Nanosheet on Ni foam	2.4	1136 F g^{-1} at 2 A g^{-1}	(122 F g^{-1} at 0.2 A g^{-1})	94% after 2000 cycles	7
Nanonet/nanoflake on stainless steel mesh	4.2	1027 F g^{-1} at 1 A g^{-1}	(468 F g^{-1} at 0.5 A g^{-1})	80% after 10000 cycles	8
Nanowire on Ni foam	3.0	2305 F g^{-1} at 8 A g^{-1}	(300 F g^{-1} at 1.0 A g^{-1})	98% after 1000 cycles	9
Hetero-structure on Ni foam	1.8	891 F g^{-1} at 1 A g^{-1}	(74 F g^{-1} at 0.1 A g^{-1})	96% after 8000 cycels	10
Nanosheets on stainless steel mesh	0.85	336 F g^{-1} at 2 A g^{-1}	(32 F g^{-1} at 0.2 A g^{-1})	87% after 3000 cycles	11
Nanowire cluster on Ni foam	3.0	2132 F g^{-1} at 10 A g^{-1}	(278 F g^{-1} at 1.3 A g^{-1})	98% after 1000 cycles	12
Nanosheets on Ni nanofoam	1.54	899 F g^{-1} at 1 A g^{-1}	--	84% after 6000 cycles	13
Nanowires on carbon textiles	1.2	1283 F g^{-1} at 1 A g^{-1}	--	100% after 5000 cycles	14

Nanowires on carbon fiber paper	0.8	471 F g^{-1} at 1 A g^{-1}	--	87% after 2500 cycles	15
Nanosheets on carbon fiber paper	0.8	799 F g^{-1} at 1 A g^{-1}	--	80% after 2500 cycles	16
Nanowires on carbon cloth	0.96	1501 F g^{-1} at ~5 A g^{-1}	--	73% after 500o cycles	16
Nanosheets on carbon foam	2.4	1140 F g^{-1} at 4 A g^{-1}	--	81% after 3000 cycles	17
Nanosheets on carbon fiber paper	0.8	1422 F g^{-1} at 1 A g^{-1}	--	84% after 3000 cycles	18
Slurry-based microsphere on Ni foam	3.0	1006 F g^{-1} at 1 A g^{-1}	(131 F g^{-1} at 0.1 A g^{-1})	93% after 1000 cylces	19
Slurry-based aerogels on graphite electrode	0.4	1400 F g^{-1} at 25 mV s^{-1}	(400 F g^{-1} at 25 mV s^{-1})	90% after 2000 cycles	20
Slurry-based nanosheets with graphene and PANI	1.0	966 F g^{-1} at 1 A g^{-1}	--	86% after 4000 cycles	21
Slurry-based nanosheets on Ni foam	1.0	560 F g^{-1} at 2 A g^{-1}	(27 F g^{-1} at 0.1 A g^{-1})	95% after 5000 cycles	22
Slurry-based hierarchical structure Ni foam	5~6	1104 F g^{-1} at 1 A g^{-1}	(221~254 F g^{-1} at 0.2 A g^{-1})	95% after 1000 cycles	23
Slurry-based nanoflake on Ni foam	2.0	1464 F g^{-1} at 4 A g^{-1}	(113 F g^{-1} at 0.4 A g^{-1})	85% after 5000 cycles	24
Slurry-based microtubes on Ni foam	1.0	1387 F g^{-1} at 2 A g^{-1}	(66 F g^{-1} at 0.1 A g^{-1})	89% after 12000 cycles	25
Slurry-based nanowires on Ni foam	8.5	401 F g^{-1} at 1 A g^{-1}	(121 F g^{-1} at 0.3 A g^{-1})	90% after 1000 cycles	26

Slurry-based nanorods on Ni foam	1.0	565 F g^{-1} at 1 A g^{-1}	(27 F g^{-1} at 0.1 A g^{-1})	77% after 1000 cycles	27
Slurry-based nanoparticles on Ni foam	1.0	1254 F g^{-1} at 2 A g^{-1}	(60 F g^{-1} at 0.1 A g^{-1})	72% after 1000 cycles	28
Slurry-based nanowires on Ni foam	5.6~10.2	564 F g^{-1} at 1 A g^{-1}	(123~190 F g^{-1} at 0.3~0.4 A g^{-1}l)	45% after 2000 cycles	29
Slurry-based nanotubes on Ni foam	1~2	1045 F g^{-1} at 5 A g^{-1}	(49~100 F g^{-1} at 0.2~0.4 A g^{-1})	71% after 10000 cycles	30
Slurry-based double-shell hollow spheres on Ni foam	3~5	568 F g^{-1} at 1 A g^{-1}	(74~114 F g^{-1} at 0.1~0.2 A g^{-1})	82% after 2000 cycles	31
Slurry-based microspheres on Ni foam	1.4	1701 F g^{-1} at 1 A g^{-1}	(111 F g^{-1} at 0.1 A g^{-1})	78% after 1000 cycles	32

[a] In the column of the specific capacitance (active materials basis), the data are adopted directly from the referred paper and based on the active materials and/or active layers without considering the mass of current collectors.

[b] In the column of the electrode-based capacitance, some specific capacitances are given in parentheses. It means that the paper indicates the type of current collectors but disclose no parameter information. We estimated their electrode-based capacitances according to the widely-used parameters of Al foil or commercial nickel foam in most literatures.

"--" means that no information is provided in the literatures. It is unable to estimate the electrode-based capacitance.

Summary of $NiCo_2O_4$ used as Li-ion battery anodes in literatures

The electrochemical reaction of $NiCo_2O_4$ as Li-ion battery anodes has been well studied. It can be summarized as follows:[14,22,33−41,43,45,48]

$$NiCo_2O_4 + 8Li^+ + 8e^- = Ni + 2Co + 4Li_2O$$

According to the above mechanism, there are 8 lithium atom involved in the lithiation process. The theoretical specific capacity of $NiCo_2O_4$ could be calculated 901 mAh g^{-1}. Li-ion batteries require metal foils (Cu for anodes and Al for cathodes) to conduct electrons because the in-plane conductivity of active material layers is usually low. Fig. S7j−l show that the Cu foil used in several typical commercial Li-ion battery anodes is around 10 μm thick. The actual specific capacity based on the electrode mass is usually lower than that based on active materials. Some current collectors such as nickel foam (due to surface oxides) or carbon cloth may contribute to the measured capacity. When the active material based capacity is used as a parameter to compare the electrode performance, the calculated capacity may be occasionally larger than the theoretic value of active materials. No matter from the scientific or practical viewpoints, the specific capacity (electrode basis) is necessary and reasonable.

In this study, we developed an ultralight nickel foam (UNF) to replace the Cu foil and conductive agents which are indispensable in the conventional Li-ion anodes. To compare on the reasonable basis, the Cu foil mass should be included in the specific capacity of electrode. Table S2 summarizes the previous reports about $NiCo_2O_4$ anodes. In the literatures, the anode current collectors are usually nickel foam, carbon cloth, Cu foil, etc. However, a very few reports disclose the mass of current collectors. Most of reports only show the specific capacity of active materials or/and conductive agents.

We have summarized the information about the areal loading, cyclability, and specific capacity in the literatures and listed them in Table S2. We estimated the electrode-based capacity by including the mass of Cu current collectors, which is obtained from the commercial batteries. We suppose that the both sides of Cu foils are coated with active materials. The mass of 5 μm thick Cu foil is included to calculate the electrode-based capacity. For the literatures using commercial nickel foam, we used the data (20 mg cm^{-2}) in the widely-cited two papers about commercial nickel foam.[2,3]

Table S2. Performance and parameters of previous reported $NiCo_2O_4$ Li-ion anodes.

$NiCo_2O_4$ Electrode Structure	Load (mg cm^{-2})	Specific capacity of the second cycle (active material basis)[a]	Specific capacity of the second cycle (electrode basis)[b]	Cyclability	Ref.
Nanowires on UNF	6.0	815 mAh g^{-1} at 0.1 A g^{-1}	612 mAh g^{-1} at 0.08 A g^{-1}	77% after 150 cycles	This work
Nanosheet on Ni foam	1.0	1343 mAh g^{-1} at 0.2 A g^{-1}	(64 mAh g^{-1} at 0.01 A g^{-1})	87% after 50 cycles	33
Nanowires on Ni foam	1.2	1009 mAh g^{-1} at 0.2 A g^{-1}	(57 mAh g^{-1} at 0.01 A g^{-1})	96% after 50 cycles	34
Nanosheets on Ni foam	3.4	780 mAh g^{-1} at 0.3 A g^{-1}	(114 mAh g^{-1} at 0.04 A g^{-1})	76% after 20 cycles	35
Nanowires on Ni foam	2.0	1602 mAh g^{-1} at 0.1 A g^{-1}	(148 mAh g^{-1} at 0.01 A g^{-1})	26% after 50 cycles	36
Coated Vertically Aligned CNTs on Cu foil	0.62	1147 mAh g^{-1} at 0.1 A g^{-1}	(138 mAh g^{-1} at 0.01 A g^{-1})	106% after 200 cycles	37
Nanowires on carbon fiber cloth	1.3~1.5	1200 mAh g^{-1} at 0.5 A g^{-1}	--	90% after 200 cycles	38
Nanowires on carbon textiles	1.2	1016 mAh g^{-1} at 0.5 A g^{-1}	--	84% after 100 cycles	14

Slurry-based nanoparticles with C foam on Cu foil	1~2	1098 mAh g^{-1} at 0.1 A g^{-1}	(200~337 mAh g^{-1} at 0.02~0.03 A g^{-1})	97% after 100 cycles	39
Slurry-based CNT composites on Cu foil	1.0	942 mAh g^{-1} at 0.3 A g^{-1}	(171 mAh g^{-1} at 0.06 A g^{-1})	108% after 200 cylces	40
Slurry-based nanosheets on Cu foil	1.0	891 mAh g^{-1} at 0.1 A g^{-1}	(162 mAh g^{-1} at 0.02 A g^{-1})	86% after 50 cycles	22
Slurry-based ultrathin nanosheets on Cu foil	1.5	1100 mAh g^{-1} at 0.2 A g^{-1}	(275 mAh g^{-1} at 0.05 A g^{-1})	78% after 100 cycles	41
Slurry-based hollow dodecahedron on Cu foil	0.4~0.6	1535 mAh g^{-1} at 0.2 A g^{-1}	(125~181 mAh g^{-1} at ~0.02 A g^{-1})	97% after 100 cycles	42
Slurry-based microspheres on Cu foil	1~1.5	1235 mAh g^{-1} at 0.2 A g^{-1}	(224~309 mAh g^{-1} at 0.04~0.05 A g^{-1})	88% after 100 cycles	43
Slurry-based nanotubes on Cu foil	1.7	1098 mAh g^{-1} at 0.1 A g^{-1}	(301 mAh g^{-1} at 0.03 A g^{-1})	44% after 200 cycles	30
Slurry-based porous ellipsoids on Cu foil	1.5	1025 mAh g^{-1} at 0.5 A g^{-1}	(257 mAh g^{-1} at 0.13 A g^{-1})	37% after 100 cycles	44
Slurry-based hollow spheres on Cu foil	--	834 mAh g^{-1} at 0.3 A g^{-1}	--	78% after 100 cycles	45
Slurry-based nanosheets on Cu foil	--	938 mAh g^{-1} at 0.2 A g^{-1}	--	38% after 50 cycles	46
Slurry-based nanoribbons on Cu foil	--	1168 mAh g^{-1} at 0.2 A g^{-1}	--	91% after 160 cycles	47

Slurry-based dried plum-like structure on Cu foil	--	1300 mAh g^{-1} at 0.1 A g^{-1}	--	96% after 50 cycles	48

[a] The specific capacity for the second cycle is used for comparison because the first cycle has low Coulomb efficiency and its irreversible capacity is high. It is more reasonable to compare the capacity for the second and last cycles here.

[b] In the column of the electrode-based capacity, the specific capacity in parentheses are estimated according to the widely-used current collector (Cu foil or commercial nickel foam).

"--" means that no information is provided in the literatures and it is unable to estimate the electrode-based capacity.

Reference

[1] S. Langlois and F. Coeuret, *J. Appl. Electrochem.*, 1989, **19**, 43−50.

[2] M. Grdeń, M. Alsabet and G. Jerkiewicz, *ACS Appl. Mater. Interfaces*, 2012, **4**, 3012−3021.

[3] V. Paserin, S. Marcuson, J. Shu and D. S. Wilkinson, *Adv. Eng. Mater.*, 2004, 6, 454−459.

[4] C. Z Yuan, J. Y Li, L. R. Hou, X. G. Zhang, L. F. Shen, and X. W. Lou, *Adv. Funct. Mater.*, 2012, **22**, 4592−4597.

[5] G. Q. Zhang and X. W. Lou, *Adv. Mater.*, 2013, **25**, 976−979.

[6] J. B. Cheng, Y. Lu, K. W. Qiu, D. Y. Zhang, C. L. Wang, H. L. Yan, J. Y. Xu, Y. H. Zhang, X. M. Liu and Y. S. Luo, *CrystEngComm*, 2014, **16**, 9735−9742

[7] D. P. Cai, S. H. Xiao, D. D. Wang, B. Liu, L. L. Wang, Y. Liu, H. Li, Y. R. Wang, Q. H. Li and T. H. Wang, *Electrochim. Acta*, 2014, **142**, 118−124.

[8] Y. Lu, H. L. Yan, D. Y. Zhang, J. Lin, Y. M. Xue, J. Li, Y. S. Luo and C. C. Tang, *J. Solid State Electrochem.*, 2014, **18**, 3143−3152.

[9] Q. F. Wang, X. F. Wang, B. Liu, G. Yu, X. J. Hou, D. Chen and G. Z. Shen, *J. Mater. Chem. A*,

2013, **1**, 2468−2473.

[10] X. Y. Liu, Y. Q. Zhang, X. H. Xia, S. J. Shi, Y. Lu, X. L. Wang, C. D. Gu and J. P. Tu, *J. Power Sources*, 2013, **239**, 157−163.

[11] Y. B. Zhang, B. Wang, F. Liu, J. P. Cheng, X. W. Zhang and L. Zhang, *Nano Energy*, 2016, **27** 627−637.

[12] Y. J. Chen, B. H. Qu, L. L. Hu, Z. Xu, Q. H. Li and T. H. Wang, *Nanoscale*, 2013, **5**, 9812−9820.

[13] G. X. Gao, H. B. Wu, S. J. Ding, L. M Liu and X. W. Lou, *Small***,** 2015, **11**, 804−808.

[14] L. F. Shen, Q. Che , H. S. Li and X. G. Zhang, *Adv. Funct. Mater.*, 2014, **24**, 2630−2637.

[15] F. Z. Deng, L. Yu, M. Sun, T. Lin, G. Cheng, B. Lan and F. Ye, *Electrochim. Acta*, 2014, **133** 382−390.

[16] W. L. Yang, Z. Gao, J. Ma, X. M. Zhang, J. Wang and J. Y. Liu, *J. Mater. Chem. A*, 2014, **2**, 1448−1457.

[17] J. Wang, L. F. Shen, P. Nie, X. L. Yun, Y. L. Xu, H. Dou and X. G. Zhang, *J. Mater. Chem. A*, 2015, **3**, 2853−2860.

[18] F. Z. Deng, L. Yu, G. Cheng, T. Lin, M. Sun, F. Ye and Y. F. Li, *J. Power Sources*, 2014, **251**, 202−207.

[19] Y. Lei, J. Li, Y. Y. Wang, L. Gu, Y. F. Chang, H. Y. Yuan and D. Xia, *ACS Appl. Mater. Interfaces*, 2014, **6**, 1773−1780.

[20] T. Y. Wei, C. H. Chen, H. C. Chien, S. Y. Lu and C. C. Hu, *Adv. Mater.*, 2010, **22**, 347−351.

[21] J. Yang, C. Yu, S. X. Liang, S. F. Li, H. W. Huang, X. T. Han, C. T. Zhao, X. D. Song, C. Hao, P. M. Ajayan and J. S. Qiu, *Chem. Mater.*, 2016, **28**, 5855−5863.

[22] A. K. Mondal, D. W. Su, S. Q. Chen, K. Kretschmer, X. Q. Xie, H. J. Ahn and G. X. Wang, *ChemPhysChem*, 2015, **16**, 169−175.

[23] S. Wang, S. M. Sun, S. D. Li, F. L. Gong, Y. N. Li, Q. Wu, P. Song, S. M. Fang and P. Y. Wang, *Dalton Trans.*, 2016, **45**, 7469−7475.

[24] Y. J. Sun, X. P. Xiao, P. J. Ni, Y. Shi, H. C. Dai, J. T. Hu, Y. L. Wang, Z. Li and Z. Li, *Electrochim. Acta*, 2014, **121**, 270−277.

[25] F. X. Ma, Le Yu, C. Y. Xu and X. W. Lou, *Energy Environ. Sci.*, 2016, **9**, 862−866.

[26] C. Z. Yuan, J. Y. Li, L. R. Hou, L. Yang, L. F. Shen and X. G. Zhang, *J. Mater. Chem.*, 2012, **22**, 16084−16090.

[27] Y. R. Zhu, X. L. Pu, W. X. Song, Z. B. Wu, Z. Zhou, X. He, F. Lu, M. J. Jing, B. Tang and X. B. Ji, *J. Alloys Comp.*, 2014, **617**, 988−993.

[28] Y. R. Zhu, X. B. Ji, Z. P. Wu, W. X. Song, H. S. Hou, Z. B. Wu, X. He, Q. Y. Chen and C. E. Banks, *J. Power Sources*, 2014, **267**, 888−900.

[29] G. Y. He, L. Wang, H. Q. Chen, X. Q. Sun and X. Wang, *Mater. Lett.*, 2013, **98**, 164−167.

[30] J. Zhu, Z. Xun and B. A. Lu, *Nano Energy*, 2014, **7**, 114−123.

[31] X. M. Li, L. F. Jiang, C. Zhou, J. P. Liu and H. B. Zeng, *NPG Asia Mater.*, 2015, **7**, e165.

[32] G. W. Chen, Y. Z. Gao and H. Zhang, *RSC Adv.*, 2016, **6**, 30488−30497.

[33] X. N Leng, Y. Shao, S. F. Wei, Z. H. Jiang, J. S. Lian, G. Y. Wang and Q. Jiang, *ChemPlusChem*, 2015, **80**, 1725−1731.

[34] Q. B. Zhang, H. X. Chen, J. X. Wang, D. G. Xu, X. H. Li, Y. Yang and K. L. Zhang, *ChemSusChem*, 2014, **7**, 2325−2334.

[35] Y. J. Chen, J. Zhu, B. H. Qu, B. A. Lun and Z. Xu, *Nano Energy*, 2014, **3**, 88−94.

[36] G. H. Chen, J. Yang, J. J. Tang and X. Y. Zhou, *RSC Adv.*, 2015, **5**, 23067−23072.

[37] W. W. Liu, C. X. Lu, K. Liang and B. K. Tay, *Part. Part. Syst. Charact.*, 2014, **31**, 1151−1157.

[38] Y. D. Mo, Q. Ru, J. F. Chen, X. Song, L. Y. Guo, S. J. Hu and S. M. Peng, *J. Mater. Chem. A*, 2015, **3**, 19765−19773.

[39] L. Y. Wang, L. H. Zhuo, C. Zhang and F. Y. Zhao, *ACS Appl. Mater. Interfaces*, 2014, **6**, 10813−10820.

[40] S. Abouali, M. A. Garakani, Z. L. Xu and J. K. Kim, *Carbon*, 2016, **102**, 262−272.

[41] Y. Q. Zhu and C. B. Cao, *Electrochim. Acta*, 2015, **176**, 141−148.

[42] C. C. Sun, J. Yang, X. H. Rui, W. N. Zhang, Q. Y. Yan, P. Chen, F. W. Huo, W. Huang and X. C. Dong, *J. Mater. Chem. A*, 2015, **3**, 8483−8488.

[43] L. Liu, H. J. Zhang, J. Yang, Y. P. Mu and Y. Wang, *J. Mater. Chem. A*, 2015, **3**, 22393−22403.

[44] Y. D. Mo, Q. Ru, X. Song, J. F. Chen, X. H. Hou, S. J. Hu and L. Y. Guo, *RSC Adv.*, 2016, **6**, 31925−31933.

[45] L. F. Shen, L. Yu, X. Y. Yu, X. G. Zhang and X. W. Lou, *Angew. Chem. Int. Ed.*, 2015, **54**, 1868−1872.

[46] Z. Y. Fan, B. R. Wang, Y. X. Xi, X. Xu, M. Y. Li, J. Li, P. Coxon, S. D. Cheng, G. X. Gao, C. H. Xiao, G. Yang, K. Xi, S. J. Ding and R. V. Kumar, *Carbon*, 2016, **99**, 633−641.

[47] B. S. Li, J. K. Feng, Y. T. Qian and S. L. Xiong, *J. Mater. Chem. A*, 2015, **3**, 10336−10344.

[48] T. Li, X. H. Li, Z. X. Wang, H. J. Guo and Y. Li, *J. Mater. Chem. A*, 2015, **3**, 11970−11975.